SEARCH FOR EXOTIC DIHIGGS PRODUCTION IN THE $hh \rightarrow b\bar{b}WW^{*}$ DECAY CHANNEL USING THE ATLAS DETECTOR

2 August 2017

APS | DIVISION OF PARTICLES & FIELDS

DPF 2017

MEETING OF THE AMERICAN PHYSICAL SOCIETY DIVISION OF PARTICLES AND FIELDS

THE OHIO STATE UNIVERSITY

ATLAS EXPERIMENT

Benjamin Tannenwald

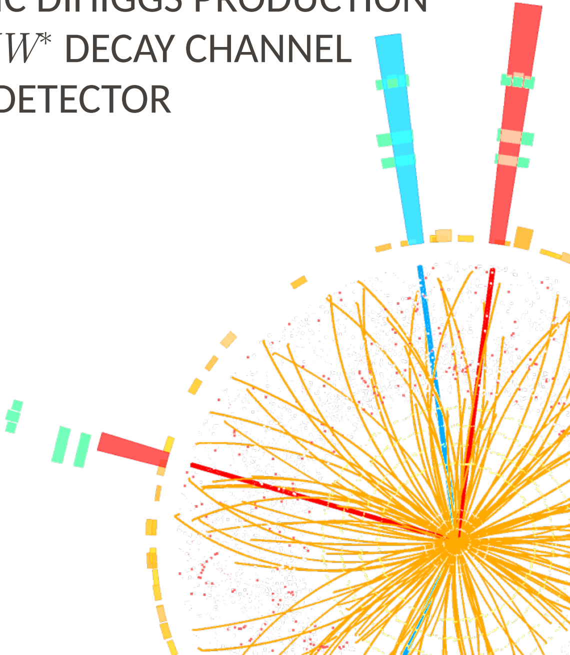

- Search for non-resonant (SM) and resonant (exotic) dihiggs production in the $b\bar{b}WW^{*}$ final state
  - Second highest branching fraction after $hh \to b\bar{b}b\bar{b}$
  - Analysis in semileptonic decay channel, i.e. $b\bar{b}WW^{*} \to b\bar{b}\ell\nu q\bar{q}$
- Three selection strategies: non-resonant, low resonant mass, high resonant mass
- Require one charged lepton (e, μ), ≥ 4 jets, = 2 b-tags
- First search using $b\bar{b}WW^{*} \to b\bar{b}\ell\nu q\bar{q}$ final state

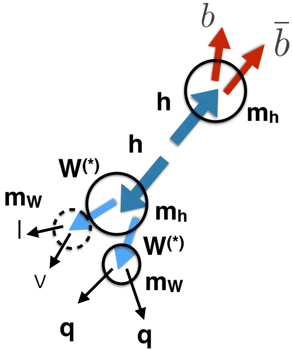

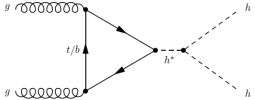

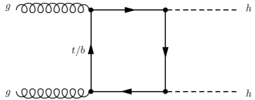

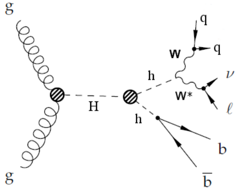

DATASET + OBJECT SELECTION

- Use 36.5 fb^{-1} of data from 13 TeV proton-proton collisions recorded by the ATLAS detector in 2015-2016
- Monte Carlo simulations used for dihiggs signal, $t\bar{t}$, W+jets, Z+jets, diboson, and single top backgrounds
  - $t\bar{t}$ normalization calculated using data in control region
- Data-driven ABCD method used to estimate multi-jet QCD background

Object Selection

Lepton: p_T^{ℓ} > 27 GeV, $|\eta^{\ell}|$ < 2.5, track-based isolation
Jets: Anti-k_T R=0.4 jets, p_T^{jet} > 20 GeV, $|\eta^{jet}|$ < 2.5, |JVF| > 0.59, 85% b-tagging efficiency
MET: MET$\geq$25 GeV

Event Selection

Lepton trigger
At least 1 primary vertex with ≥ 5 tracks
$N_{\ell} = 1$
$N_{jets} \geq 4$
Categorize by $N_{b\text{-tags}} = 2$

- Create $m_{b\bar{b}}$ control region ($m_{b\bar{b}} < 100$, $m_{b\bar{b}} > 140$ GeV) to validate techniques and optimize search strategies for resonant and non-resonant hh production
- Blind signal region ($100 < m_{b\bar{b}} < 140$ GeV) to avoid bias

EVENT RECONSTRUCTION

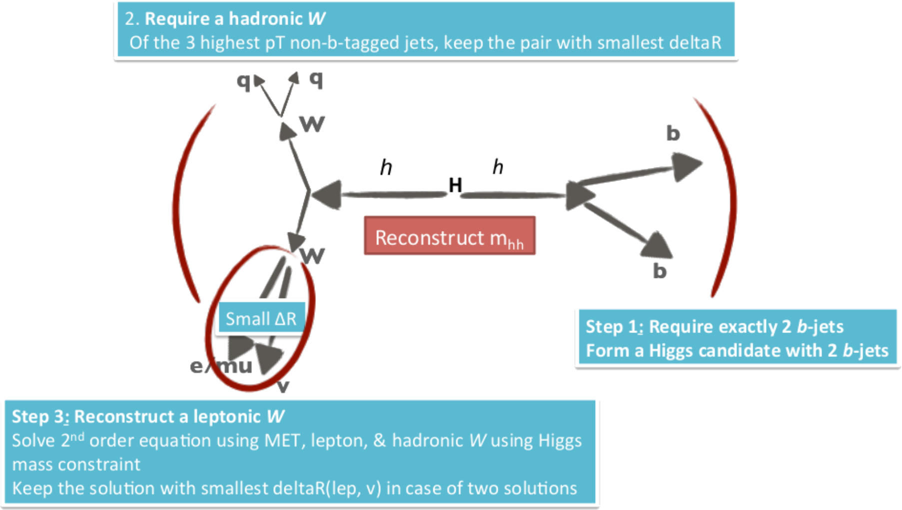

Largest background contributions come from $t\bar{t}$ and multi-jet processes

EVENT SELECTION

Variable	Non-resonant	Low-mass	High-mass
MET [GeV]	> 25		
p_{T}^{WW} [GeV]	> 250		
m$_{b\bar{b}}$ [GeV]	$105 - 135$		
m$_{WW}$ [GeV]	< 130	< 130	no cut
$p_{\mathrm{T}}^{b\bar{b}}$ [GeV]	> 300	> 210	> 350
ΔR$_{WW}$	no cut	no cut	< 1.5
m$_{hh}$ [GeV]	no cut	$[625, 775]^{\dagger}$	$[1910, 2170]^{\dagger}$

→ Selection variables differ between analysis strategies

- → Variables and cuts chosen by calculating Poisson signifiance (including systematics) at end of each selection

→ † - m$_{hh}$ cuts are dependent on resonance mass under consideration

- → Two cut windows are shown above for for 700 GeV (low-mass) resonance and 2000 GeV (high-mass) resonance

QCD ESTIMATION: ABCD METHOD

→ Multi-jet backgrounds enter event selection due to jets mis-identified as leptons and non-prompt lepton production

→ Such processes not well-modeled by simulation, so use data-driven ABCD method to estimate contributions in selected phase space

→ ABCD estimation is a 2D sideband method where the signal region, A, has two (uncorrelated) cuts inverted to create three independent control regions

→ Using $|d_0/\sigma_{d_0}|$ and MET as independent ABCD variables

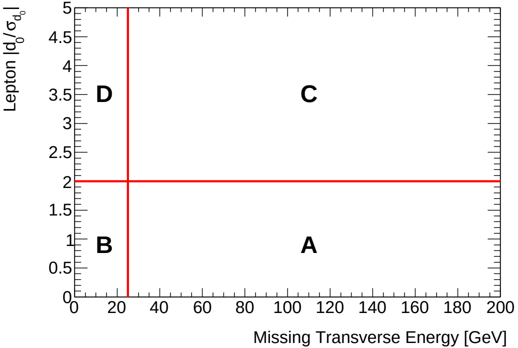

→ A region: $|d_0/\sigma_{d_0}| <$2.0 and MET $>$ 25 GeV

→ B region: $|d_0/\sigma_{d_0}| <$2.0 and MET $<$ 25 GeV

→ C region: $|d_0/\sigma_{d_0}| >$2.0 and MET $>$ 25 GeV

→ D region: $|d_0/\sigma_{d_0}| >$2.0 and MET $<$ 25 GeV

QCD ESTIMATION: ABCD CALCULATION

To estimate $N_A^{\text{non-prompt}}$ ($N_i^{\text{non-prompt}} = N_i^{\text{Data}} - N_i^{\text{All MC Bkgs}}$), the following formula is used:

$$N_A^{\text{non-prompt}} = R \cdot N_C^{\text{non-prompt}} \cdot \frac{N_B^{\text{non-prompt}}}{N_D^{\text{non-prompt}}}$$

→ Assumption is that difference in behavior between B and D regions is identical to difference between A and C regions

→ Ratio after 1st cut $\frac{N_A^{\text{non-prompt}} N_D^{\text{non-prompt}}}{N_B^{\text{non-prompt}} N_C^{\text{non-prompt}}} \equiv R$ applied to subsequent QCD yields

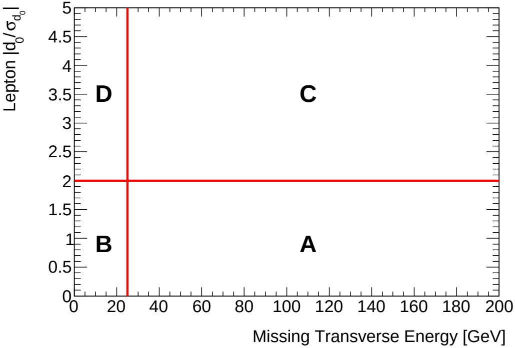

→ QCD (non-prompt) shape in C region taken to be shape in A region

→ Freeze B and D regions at early stage in cutflow to reduce statistical error in final estimation

CONTROL REGION KINEMATICS (NON-RESONANT + LOW-MASS)

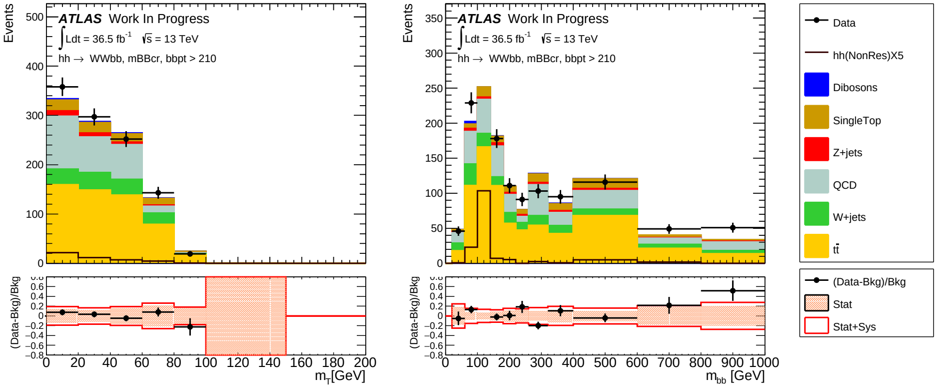

→ Distributions above in m$_{b\bar{b}}$ control region after requiring m$_{WW} < 130$ GeV and $p_{\mathrm{T}}^{b\bar{b}} > 210$ GeV

→ m$_{\mathrm{T}}^{W}$ (left) shows Data/Bkg agreement consistent within error using ABCD estimation

→ m$_{b\bar{b}}$ (right) shows backgrounds well modeled in m$_{b\bar{b}}$ sideband

CONTROL REGION KINEMATICS (HIGH MASS)

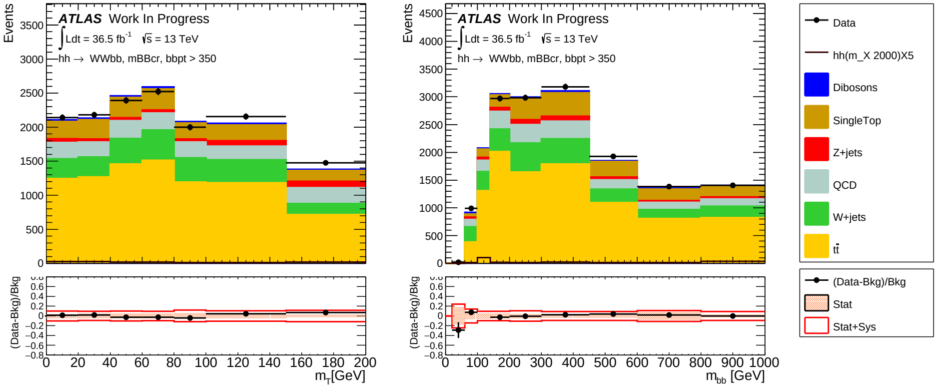

→ Distributions above in $m_{b\bar{b}}$ control region after requiring $p_T^{b\bar{b}} > 350$ GeV

→ m_T^W (left) shows Data/Bkg agreement consistent within error using ABCD estimation

→ $m_{b\bar{b}}$ (right) shows backgrounds well modeled in $m_{b\bar{b}}$ sideband

CONTROL REGION EVENT YIELDS: NON-RESONANT

Sample	$m_{WW} < 130$	$p_T^{bb} > 210$	$p_T^{bb} > 300$	$p_T^{WW} > 250$	$m_{b\bar{b}}$ Window
Top Control Region: $m_{b\bar{b}}$ Sideband					
$t\bar{t}$	23776.6 ± 87.2	531.7 ± 13.1	109.9 ± 5.9	63.9 ± 4.6	0.0 ± 0.0
QCD	13310.5 ± 500.3	250.2 ± 30.6	33.7 ± 4.1	21.4 ± 2.6	0.0 ± 0.0
W+jets	3938.9 ± 31.1	124.7 ± 3.5	29.3 ± 1.4	17.1 ± 1.1	0.0 ± 0.0
Single Top	1605.4 ± 18.0	76.0 ± 3.8	20.1 ± 2.0	13.5 ± 1.7	0.0 ± 0.0
Diboson	109.9 ± 2.7	8.3 ± 0.8	2.2 ± 0.4	1.5 ± 0.4	0.0 ± 0.0
Z+jets	1107.6 ± 8.4	27.1 ± 0.8	6.7 ± 0.4	2.4 ± 0.2	0.0 ± 0.0
Background Sum	43849.0 ± 509.2	1017.9 ± 33.7	201.9 ± 7.6	119.8 ± 5.7	0.0 ± 0.0
Non-resonant hh	44.6 ± 2.2	9.1 ± 0.7	1.5 ± 0.2	1.1 ± 0.1	0.0 ± 0.0
Data	43902.0	1069.0	206.0	138.0	0.0
Signal Region: $100 < m_{b\bar{b}} < 140$ GeV					
$t\bar{t}$	7461.0 ± 48.6	162.9 ± 7.3	27.9 ± 2.9	18.4 ± 2.4	15.4 ± 2.2
QCD	2756.2 ± 210.5	48.7 ± 14.2	6.6 ± 1.9	4.2 ± 1.2	3.6 ± 1.6
W+jets	640.8 ± 12.7	19.1 ± 1.4	5.0 ± 0.6	3.1 ± 0.5	2.3 ± 0.4
Single Top	452.2 ± 9.6	14.3 ± 1.7	1.7 ± 0.5	1.0 ± 0.4	0.6 ± 0.3
Diboson	21.6 ± 1.3	0.6 ± 0.2	0.4 ± 0.2	0.0 ± 0.0	0.0 ± 0.0
Z+jets	262.8 ± 4.4	3.1 ± 0.3	1.0 ± 0.2	0.2 ± 0.1	0.2 ± 0.1
Background Sum	11594.7 ± 216.7	248.6 ± 16.1	42.6 ± 3.6	27.0 ± 2.8	22.1 ± 2.8
Non-resonant hh	68.3 ± 2.4	20.7 ± 0.9	6.7 ± 0.4	5.5 ± 0.3	4.8 ± 0.3
Data	—	—	—	—	—

- → RED is $m_{b\bar{b}}$ control region, BLUE is final signal region
- → Non-resonant signal normalized to ATLAS 8 TeV upper limit (0.59 pb)
- → Uncertainties are statistical only

CONTROL REGION EVENT YIELDS: LOW-MASS

Top Control Region: m$_{b\bar{b}}$ Sideband					
Sample	m$_{WW} < 130$	$p_{\mathrm{T}}^{bb} > 210$	$p_{\mathrm{T}}^{WW} > 250$	m$_{hh}$ Window	m$_{b\bar{b}}$ Window
$t\bar{t}$	23776.6 ± 87.2	531.7 ± 13.1	175.6 ± 7.5	34.4 ± 3.3	0.0 ± 0.0
QCD	13310.5 ± 500.3	250.2 ± 30.6	72.4 ± 8.9	16.3 ± 2.0	0.0 ± 0.0
W+jets	3938.9 ± 31.1	124.7 ± 3.5	45.7 ± 2.1	8.7 ± 1.1	0.0 ± 0.0
Single Top	1605.4 ± 18.0	76.0 ± 3.8	28.4 ± 2.4	5.1 ± 1.0	0.0 ± 0.0
Diboson	109.9 ± 2.7	8.3 ± 0.8	2.8 ± 0.5	0.5 ± 0.2	0.0 ± 0.0
Z+jets	1107.6 ± 8.4	27.1 ± 0.8	5.8 ± 0.4	1.2 ± 0.2	0.0 ± 0.0
Background Sum	43849.0 ± 509.2	1017.9 ± 33.7	330.7 ± 12.1	66.2 ± 4.1	0.0 ± 0.0
$m_H = 700$	4.2 ± 0.2	2.2 ± 0.1	1.5 ± 0.1	0.6 ± 0.1	0.0 ± 0.0
Data	43902.0	1069.0	367.0	89.0	0.0
Signal Region: $100 <$ m$_{b\bar{b}} < 140$ GeV					
$t\bar{t}$	7461.0 ± 48.6	162.9 ± 7.3	61.5 ± 4.7	12.4 ± 1.9	7.6 ± 1.4
QCD	2756.2 ± 210.5	48.7 ± 14.2	14.1 ± 4.1	3.2 ± 0.9	2.8 ± 1.2
W+jets	640.8 ± 12.7	19.1 ± 1.4	9.7 ± 1.1	2.9 ± 0.6	1.6 ± 0.4
Single Top	452.2 ± 9.6	14.3 ± 1.7	2.6 ± 0.7	0.5 ± 0.2	0.3 ± 0.2
Diboson	21.6 ± 1.3	0.6 ± 0.2	0.2 ± 0.1	0.2 ± 0.1	0.2 ± 0.1
Z+jets	262.8 ± 4.4	3.1 ± 0.3	0.6 ± 0.1	0.1 ± 0.0	0.1 ± 0.0
Background Sum	11594.7 ± 216.7	248.6 ± 16.1	88.7 ± 6.4	19.2 ± 2.2	12.6 ± 1.9
$m_H = 700$	9.2 ± 0.3	7.8 ± 0.2	5.9 ± 0.2	3.8 ± 0.2	3.4 ± 0.2
Data	—	—	—	—	—

→ RED is m$_{b\bar{b}}$ control region, BLUE is final signal region

→ Resonant $m_H = 700$ GeV cross-section normalized to ATLAS 8 TeV upper limit (0.044 pb)

→ Uncertainties are statistical only

CONTROL REGION EVENT YIELDS: HIGH-MASS

Top Control Region: $m_{b\bar{b}}$ Sideband					
Sample	$p_T^{bb} > 350$	$p_T^{WW} > 250$	$\Delta R_{WW} < 1.5$	m_{hh} Window	m_{bb} Window
$t\bar{t}$	8568.7 ± 52.1	7095.6 ± 47.5	1940.5 ± 25.1	122.3 ± 6.5	0.0 ± 0.0
QCD	1538.7 ± 252.7	1359.5 ± 75.9	392.7 ± 21.9	20.7 ± 1.2	0.0 ± 0.0
W+jets	2259.5 ± 7.9	1952.1 ± 7.4	696.6 ± 4.6	55.5 ± 1.1	0.0 ± 0.0
Single Top	1778.1 ± 19.4	1601.6 ± 18.4	405.4 ± 9.2	29.6 ± 2.6	0.0 ± 0.0
Diboson	170.6 ± 3.9	147.1 ± 3.7	46.8 ± 2.1	3.4 ± 0.6	0.0 ± 0.0
Z+jets	403.6 ± 2.1	307.6 ± 1.8	95.6 ± 1.1	7.5 ± 0.3	0.0 ± 0.0
Background Sum	14719.1 ± 258.9	12463.5 ± 91.8	3577.5 ± 35.0	238.9 ± 7.2	0.0 ± 0.0
$m_H = 2000$ GeV	25.7 ± 0.4	24.0 ± 0.4	9.6 ± 0.3	2.9 ± 0.1	0.0 ± 0.0
Data	14862.0	12450.0	3761.0	250.0	0.0
Signal Region: $100 < m_{b\bar{b}} < 140$ GeV					
$t\bar{t}$	1307.8 ± 20.2	1024.9 ± 17.7	287.5 ± 9.4	2.2 ± 0.8	1.4 ± 0.6
QCD	207.2 ± 99.5	191.2 ± 29.0	55.2 ± 8.4	2.9 ± 0.4	2.2 ± 0.5
W+jets	341.3 ± 3.4	291.5 ± 3.2	110.7 ± 2.1	4.8 ± 0.3	3.4 ± 0.3
Single Top	144.1 ± 5.6	126.6 ± 5.3	29.2 ± 2.6	0.5 ± 0.3	0.5 ± 0.3
Diboson	25.9 ± 1.5	21.8 ± 1.3	6.6 ± 0.7	0.0 ± 0.0	0.0 ± 0.0
Z+jets	53.8 ± 0.8	40.4 ± 0.7	13.2 ± 0.4	0.8 ± 0.1	0.7 ± 0.1
Background Sum	2080.1 ± 101.8	1696.5 ± 34.6	502.5 ± 13.1	11.2 ± 1.0	8.2 ± 0.8
$m_H = 2000$ GeV	21.0 ± 0.4	19.3 ± 0.4	8.4 ± 0.2	3.4 ± 0.1	2.9 ± 0.1
Data	—	—	—	—	—

→ RED is $m_{b\bar{b}}$ control region, BLUE is final signal region

→ Resonant $m_H = 2000$ GeV cross-section normalized to ATLAS 8 TeV upper limit (0.041 pb)

→ Uncertainties are statistical only

DOMINANT SYSTEMATICS

- → Non-resonant analysis
  - → $t\bar{t}$: normalization, ISR/FSR modeling
  - → QCD normalization
  - → Jet energy scale
  - → MET resolution
- → Low mass analysis
  - → $t\bar{t}$: normalization, parton shower modeling
  - → Jet energy scale, energy resolution
  - → QCD normalization
  - → MET resolution
- → High mass analysis
  - → W+jets: normalization, scale/PDF uncertainties
  - → QCD normalization
  - → Jet energy scale, energy resolution

LIMIT SETTING: GENERAL

- → A simultaneous maximum-likelihood fit is performed using the number of events in the final signal and control regions
- → Fit takes seven samples as input: hh signal, W+jets, Z+jets, $t\bar{t}$, single top, diboson, and multi-jet
- → $t\bar{t}$ and multi-jet normalizations factors in global fit constrained using data while diboson, W+jets, and Z+jets normalizations constrained with Gaussian priors using their SM cross-sections
- → Additional systematic uncertainties handled as Gaussian nuisance parameters in the global fit
- → Upper limits determined for the cross section of resonant $H \to hh$ production for H masses ranging from 500 to 3000 GeV
- → Upper limit on the non-resonant production of hh pairs also produced

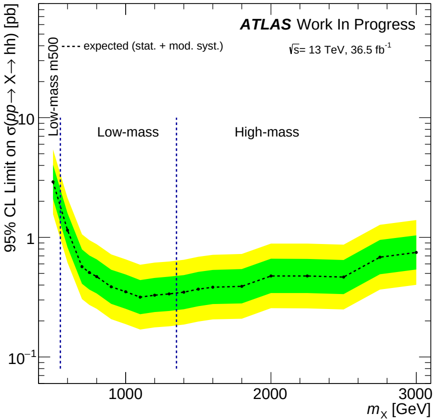

→ Resonant: most stringent expected limits for dihiggs production from the decay of an exotic resonance H is found at $\sim$0.30 pb for H masses from 900 to 1400 GeV

→ Non-resonant: expected upper limit for non-resonant dihiggs production is found to be $8.06^{+3.17}_{-2.25}$ pb

CONCLUSIONS

- → Presented search for resonant and non-resonant dihiggs production in semileptonic $b\bar{b}WW^{*}$ channel
  - → First search using $b\bar{b}WW^{*} \to b\bar{b}\ell\nu q\bar{q}$ channel
    - → Expected limits comparable with dileptonic $b\bar{b}WW^{*}$ CMS limits below 900 GeV
    - → First $b\bar{b}WW^{*}$ analysis to search for resonance masses above 900 GeV
  - → Major backgrounds ($t\bar{t}$, W+jets, multi-jet) reasonably well-controlled
  - → Expected upper limits produced for resonant $H \to hh$ production for resonance masses from 500 to 3000 GeV
  - → Expected upper limit on non-resonant hh production $8.06^{+3.17}_{-2.25}$ pb
- → Future improvements
  - → Add dileptonic and fully hadronic $b\bar{b}WW^{*}$ final states
  - → Use kinematic fitting to reject $t\bar{t}$ background / increase signal efficency
  - → Add boosted topology to increase sensitivity at high end of resonant spectrum

BACKUP SLIDES

FINAL $M_{b\bar{b}}$ DISTRIBUTIONS

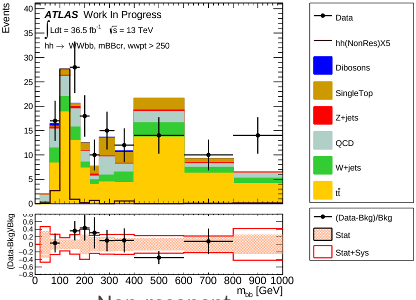

Non-resonant

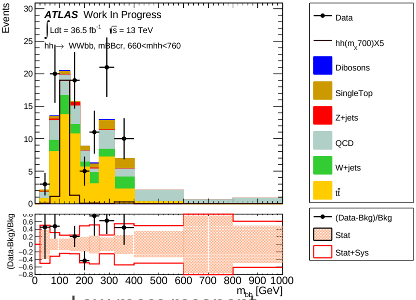

Low mass resonant

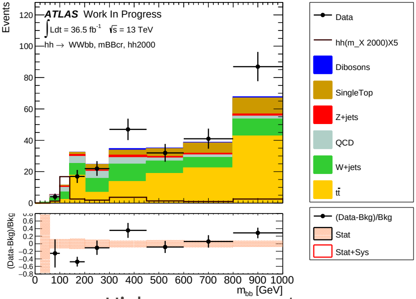

High mass resonant

QCD C REGION SHAPES

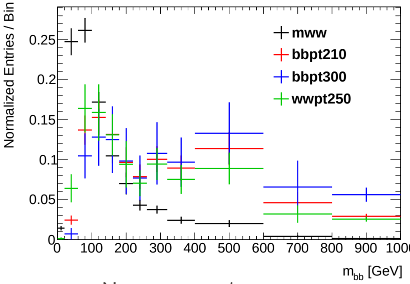

Non-resonant

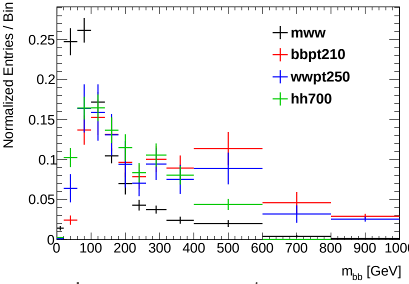

Low mass resonant

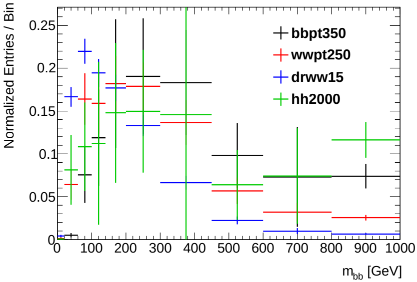

High mass resonant

LIMIT SETTING: PULL + RANKING

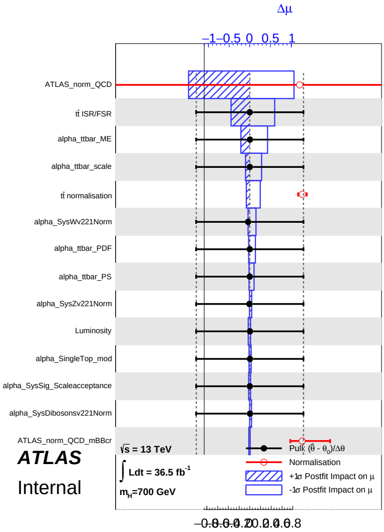

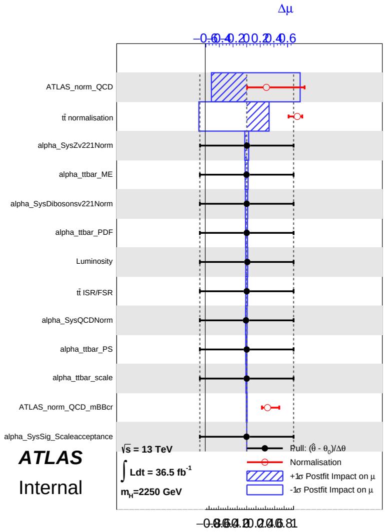

→ Systematics affecting $t\bar{t}$ and QCD normalization dominant at low mass

→ Systematics affecting W+jets more dominant at high-mass since background relatively more significant

CONSIDERED SYSTEMATICS

- → Object systematics
  - → Electrons: p_{T} resolution and scale, isolation/reconstruction/trigger/ID efficiency
  - → Muons: p_{T} resolution (MS and ID) and scale, isolation/reconstruction/trigger efficiency
  - → Jets: jet energy scale, enery resolution, jet vertex fraction
  - → b-tagging: light/c/b scale factors
  - → MET: scale, resolution
- → Modeling systematics
  - → $t\bar{t}$: PDF, scale, ISR/FSR
  - → Single top: cross-section, diagram subtraction/removal
  - → W/Z+jets: cross-section, additional jet uncertainty
  - → Diboson: cross-section, additional jet uncertainty
  - → QCD: method uncertainty evaluated using Sherpa multi-b sample